Studies of lincosamide formation complete the biosynthetic pathway for lincomycin A

Shao-An Wang[a,1], Chia-I Lin[a,1], Jiawei Zhang[a], Richiro Ushimaru[a,2], Eita Sasaki[a,3], and Hung-wen Liu[a,b,4]

[a]Department of Chemistry, The University of Texas at Austin, Austin, TX 78712; and [b]Division of Chemical Biology & Medicinal Chemistry, College of Pharmacy, The University of Texas at Austin, Austin, TX 78712

Edited by Chi-Huey Wong, Academia Sinica, Taipei, Taiwan, and approved August 20, 2020 (received for review May 10, 2020)

The structure of lincomycin A consists of the unusual eight-carbon thiosugar core methyllincosamide (MTL) decorated with a pendent *N*-methylprolinyl moiety. Previous studies on MTL biosynthesis have suggested GDP-D-*erythro*-α-D-*gluco*-octose and GDP-D-α-D-lincosamide as key intermediates in the pathway. However, the enzyme-catalyzed reactions resulting in the conversion of GDP-D-*erythro*-α-D-*gluco*-octose to GDP-D-α-D-lincosamide have not yet been elucidated. Herein, a biosynthetic subpathway involving the activities of four enzymes—LmbM, LmbL, CcbZ, and CcbS (the LmbZ and LmbS equivalents in the closely related celesticetin pathway)—is reported. These enzymes catalyze the previously unknown biosynthetic steps including 6-epimerization, 6,8-dehydration, 4-epimerization, and 6-transamination that convert GDP-D-*erythro*-α-D-*gluco*-octose to GDP-D-α-D-lincosamide. Identification of these reactions completes the description of the entire lincomycin biosynthetic pathway. This work is significant since it not only resolves the missing link in octose core assembly of a thiosugar-containing natural product but also showcases the sophistication in catalytic logic of enzymes involved in carbohydrate transformations.

lincomycin | biosynthesis | lincosamide | celesticetin | thiosugar

Lincomycins (**1** and **2**) (1–6), Bu-2545 (**3**) (7, 8), desalicetin (**4**), and celesticetin (**5**) (9, 10) are lincosamide-type antibiotics with activity against Gram-positive bacteria (Fig. 1*A*). Lincomycin A in particular can block bacterial protein synthesis by binding to the peptidyltransferase domain of the 50S ribosomal subunit due to its structural resemblance to the 3′-end of L-Pro-Met-transfer RNA (tRNA) and deacetylated tRNA (11, 12). Lincomycins have been used clinically to treat bacterial infections in patients who cannot use penicillin, cephalosporin, and macrolide antibiotics (13).

The structures of lincosamide-type antibiotics are characterized by an atypical thiooctose core (alkylthiolincosamide, **6**) decorated with a pendant alkylproline moiety. These unique structural features and their biosynthesis have recently drawn the interest of natural product chemists (14–18). The genes required for lincomycin A biosynthesis (*lmb* cluster) have been isolated and sequenced in *Streptomyces lincolnensis* strains 78–11 (19) and American Type Culture Collection (ATCC) 25466 (20). The biosynthetic gene cluster (*ccb* cluster) for celesticetin has also been identified and is publicly available. Both clusters are highly homologous (Fig. 1*B*). Previous studies have shown that the octose backbone of **1** is constructed via a *trans*-aldol reaction catalyzed by LmbR in which D-ribose 5-phosphate (**7**) serves as the C_5 acceptor, and either D-fructose 6-phosphate (**8**) or D-sedoheptulose 7-phosphate (**9**) serves as the C_3 donor (15). This is followed by 1,2-tautomerization of the resulting adduct mediated by LmbN to give the octose 8-phosphate **10** (15–21). Subsequent transformations catalyzed by LmbP, LmbK, and LmbO lead to the key intermediate, GDP-D-*erythro*-α-D-*gluco*-octose (**11**) (Fig. 2*A*) (16).

In a separate effort, Zhao et al. (17) demonstrated that sulfur incorporation is initiated by the LmbT-catalyzed substitution of GDP in **12** with ergothioneine (EGT) (**13**) to yield **14**. The ensuing N^6-amidation that produces **15** is mediated by LmbC, LmbN, and LmbD (19, 22–30). As shown in Fig. 2*A*, the final maturation steps include displacement of EGT in **15** with mycothiol (MSH) (**16**) catalyzed by LmbV to yield **17**, *N*-methylation of proline in **17** catalyzed by LmbJ along with LmbE-catalyzed hydrolysis of the MSH moiety to give **18** (17), elimination of pyruvate and ammonium from **18** catalyzed by the pyridoxal 5′-phosphate (PLP)-dependent LmbF to generate **19** (31–33), and *S*-methylation of **19** catalyzed by LmbG to complete the assembly of lincomycin A (**1**). An analogous pathway is believed to be operant in celesticetin biosynthesis. Thus, the complete biosynthetic pathway of lincomycin formation is essentially fully established with the exception of the subpathway responsible for the conversion of GDP-octose (**11**) to GDP-D-α-D-lincosamide (**12**).

It was hypothesized that the conversion of **11** to **12** would require a minimum of three reactions as shown in Fig. 2*B*, namely, C4 epimerization, C6-C8 dehydration, and C6 transamination. Among the few genes left uncharacterized in the *lmb* cluster (Fig. 1*B*), the *lmbS* gene, which is annotated to encode a PLP-dependent transaminase of the DegT/DnrJ/EryC1/StrS family (*SI Appendix*, Table S1, 62% identity [I]/73% similarity [S]), was hypothesized to be responsible for the C6 transamination

Significance

Lincomycin A is an antibiotic used clinically in the treatment of Gram-positive bacterial infections. Its biosynthesis has attracted much attention due to its unique sulfur-containing thiooctose core. Despite significant progress in our understanding of lincomycin biosynthesis, the mechanism by which GDP-D-*erythro*-α-D-*gluco*-octose maturates to GDP-D-α-D-lincosamide remains obscure. Herein, the long-sought missing link is established to consist of two epimerizations: a 6,8-dehydration and a transamination reaction catalyzed by four enzymes. Furthermore, unlike other epimerases that function regiospecifically, a single enzyme is found to catalyze epimerization at two different loci. Also, the dehydration is shown to be an α,γ-dehydration catalyzed by two enzymes. This study thus completes the description of the lincomycin biosynthetic pathway and highlights the complex mechanistic subtleties of unusual sugar biosynthesis.

Author contributions: S.-A.W., C.-I.L., and H.-w.L. designed research; S.-A.W., C.-I.L., J.Z., R.U., and E.S. performed research; S.-A.W., C.-I.L., J.Z., R.U., E.S., and H.-w.L. analyzed data; and S.-A.W., C.-I.L., and H.-w.L. wrote the paper.

The authors declare no competing interest.

This article is a PNAS Direct Submission.

[1]S.-A.W. and C.-I.L. contributed equally to this work.

[2]Present address: Laboratory of Natural Products Chemistry, Graduate School of Pharmaceutical Sciences, The University of Tokyo, 113-0033 Tokyo, Japan.

[3]Present address: Department of Applied Biological Chemistry, Graduate School of Agricultural and Life Sciences, The University of Tokyo, 113-8657 Tokyo, Japan.

[4]To whom correspondence may be addressed. Email: h.w.liu@mail.utexas.edu.

This article contains supporting information online at https://www.pnas.org/lookup/suppl/doi:10.1073/pnas.2009306117/-/DCSupplemental.

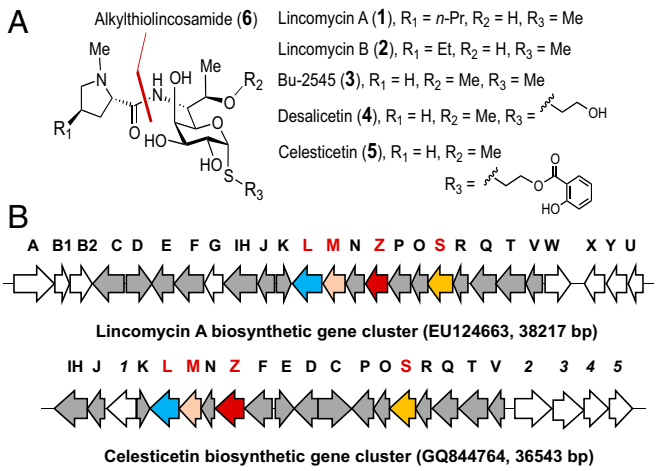

Fig. 1. (*A*) Structures of lincosamide antibiotics. (*B*) Biosynthetic gene clusters of lincomycin A (**1**) and celesticetin (**5**). Homologous genes found in both clusters (*lmb* and *ccb*) are shown in gray. Genes in color are the focus of this study. All of the white genes represent ORFs that are not directly necessary for the biosynthesis of the octose core.

(e.g., **20** → **21** or **23** → **12**). The *lmbL* and *lmbZ* genes display sequence homology to UDP-D-glucose/GDP-D-mannose 6-dehydrogenase (52%[I]/62%[S]) and members of the Gfo/Idh/MocA family of NAD(P)-dependent oxidoreductase (58%[I]/66%[S]) (*SI Appendix*, Table S1), respectively, and could thus be involved in the dehydration of the C6-C8 side chain (e.g., **11** → **20** or **22** → **23**), which may proceed via the coupling of C6 oxidation with C8 deoxygenation reactions. Finally, the *lmbM* gene resembles that encoding NAD^+-dependent UDP-D-glucose 4-epimerase (32%[I]/47%[S]) (34–37) (*SI Appendix*, Table S1) and may thus encode the corresponding 4-epimerase in the lincomycin A pathway (e.g., **11** → **22**, **20** → **23**, **21** → **12**).

As inferred above, in this pathway, dehydration of the C6-C8 side chain is hypothesized to involve two sequential redox reactions beginning with the dehydrogenation of C6–OH that leads to lowing the pK_a of C7–H in order to facilitate the elimination of the C8 hydroxyl group. This is followed by reduction of the resulting enol intermediate to complete the C8 deoxygenation. Because the resulting 6-oxo intermediate (**20** or **23**) would be the precursor to C6 transamination, dehydration should occur early in the conversion of **11** to **12**. In contrast, epimerization of C4 may take place at any stage during the transformation (Fig. 2*B*). To gain insight into the maturation process of the lincosamide core, in vitro experiments were carried out to investigate the catalytic functions of LmbM, LmbL, CcbZ, and CcbS (the latter two being homologs of LmbZ and LmbS). Interestingly, these enzymes that utilize such deceptively simple chemistry have evolved a catalytic cycle with a more complex mechanism than originally surmised. Overall, the results reported herein not only resolve the missing link in octose core assembly and thereby complete the entire lincomycin biosynthetic pathway, but also showcase the intricacy of carbohydrate conversions in natural product biosynthesis.

Results and Discussion

The genes *lmbL* and *lmbM* were heterologously expressed in *Escherichia coli*, and LmbL and LmbM were purified as *C*-His_6–tagged proteins in order to test the proposed pathway (*SI Appendix*, Table S2, and Fig. 1). The gene products CcbZ and CcbS from the celesticetin biosynthetic gene cluster are homologous to LmbZ and LmbS, respectively (*SI Appendix*, Table S1) (19, 20). CcbZ and CcbS were thus prepared in lieu of LmbZ and LmbS (*SI Appendix*, Fig. S1) because the latter could only be obtained as inclusion bodies when *lmbZ* and *lmbS* were overexpressed in *E. coli*. Compound **11**, which was synthesized in a previous work (16), was incubated separately with LmbM, LmbL, and CcbZ to determine which enzyme catalyzes the first transformation of **11** in the pathway (Fig. 2*B*). Excess NAD^+ was routinely added to assay mixtures to ensure a sufficient supply of NAD^+ for the proposed enzyme-catalyzed reactions. The reactions involved mixing 100 μM **11** and 50 μM NAD^+ with 2.5 μM of each enzyme alone or a 1:1 molar mixture of two enzymes in different combinations in 100 mM Tris buffer (pH 8.0) at room temperature for 30 min or 1 h. After incubation, the enzymes were removed by centrifugal filtration using YM-10 filters. The filtrate was then analyzed by High-Performance Liquid Chromatography (HPLC) using a Dionex CarboPac PA1 analytical column (*Materials and Methods*). As shown in Fig. 3*A*, consumption of

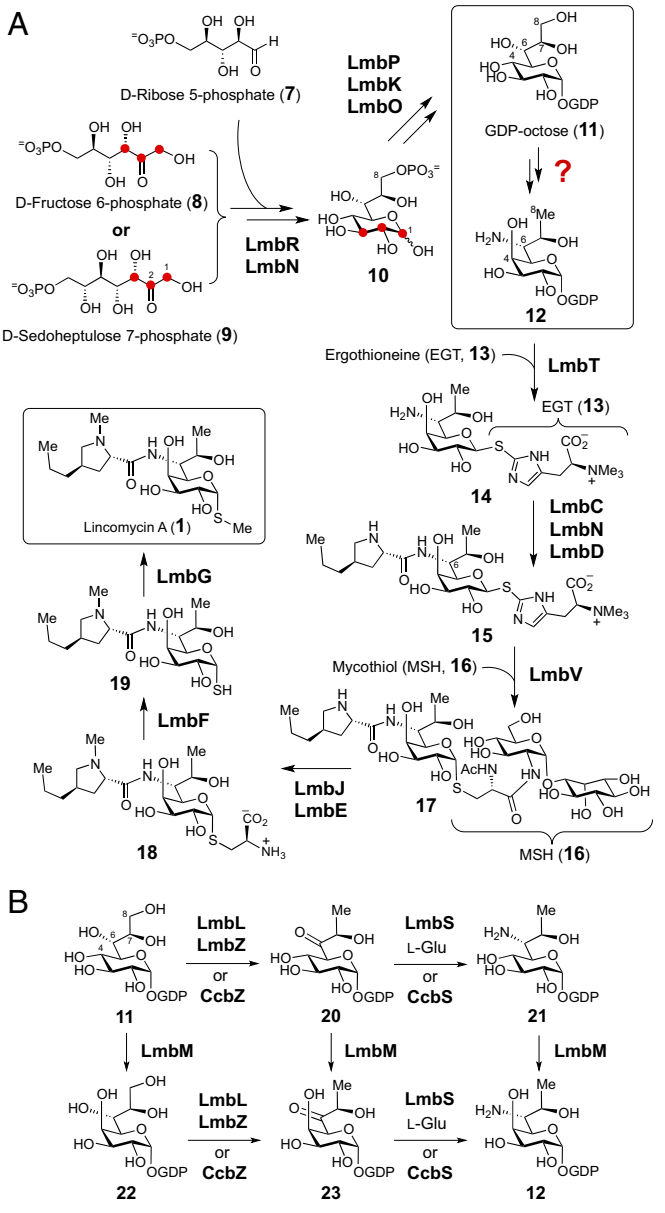

Fig. 2. (*A*) Enzymes involved in the biosynthesis of lincomycin A (**1**). (*B*) Possible reaction sequences of enzymatic conversion of **11** to **12**.

11 with concomitant formation of a new product was observed only in the presence of LmbM (Fig. 3*A*, trace *2*).

Production of this product was also noted when LmbM was incubated along with LmbL and/or CcbZ (Fig. 3*A*, traces *5* and *6*). The latter results suggested that neither LmbL nor CcbZ can catalyze consumption of the LmbM product. The LmbM product is an isomer of **11**, since both compounds have the same molecular weight (calculated [calcd] for $C_{18}H_{29}N_5O_{18}P_2$ $[M-H]^-$: 664.0910; observed [obsd]: 664.0923 for LmbM product; and 664.1078 for **11**). However, this product did not coelute with a prepared standard of GDP-D-*erythro*-α-D-*galacto*-octose (**22**) (*SI Appendix*, S2.3) upon HPLC analysis (*SI Appendix*, Fig. S2). Further analysis by NMR revealed that the isolated LmbM product retains the α-D-*gluco*-pyranose skeleton with a coupling constant of $J_{1,2} = 3.0$ Hz between H1 and H2, and a set of large coupling constants of 9.6 Hz for H2/H3, H3/H4, and H4/H5 consistent with diaxial arrangements of the latter C–H bonds (*SI Appendix*, Fig. S3). These results indicated that LmbM catalyzes either a C6 or C7 epimerization of **11** (Fig. 4) as the first step in the conversion of **11** to **12** rather than the anticipated C4 epimerization according to gene annotation of LmbM.

Accordingly, the LmbM product was hypothesized to be **24a** or **24b** (Fig. 4). However, the H6, H7, and H8 signals of **24** (**a** or **b**) overlap among themselves and with others in the NMR spectrum and cannot be fully distinguished. To resolve these signals, the C6- and C7-deuterated isotopologues of **11** (i.e., compounds [6-^{2}H]-**11** and [7-^{2}H]-**11**, respectively) were synthesized (*SI Appendix*, S2.7 and S2.8) and incubated with LmbM as described above, and the resulting products were characterized by ^{1}H NMR (*SI Appendix*, Fig. S4). Retention of the deuterium label at

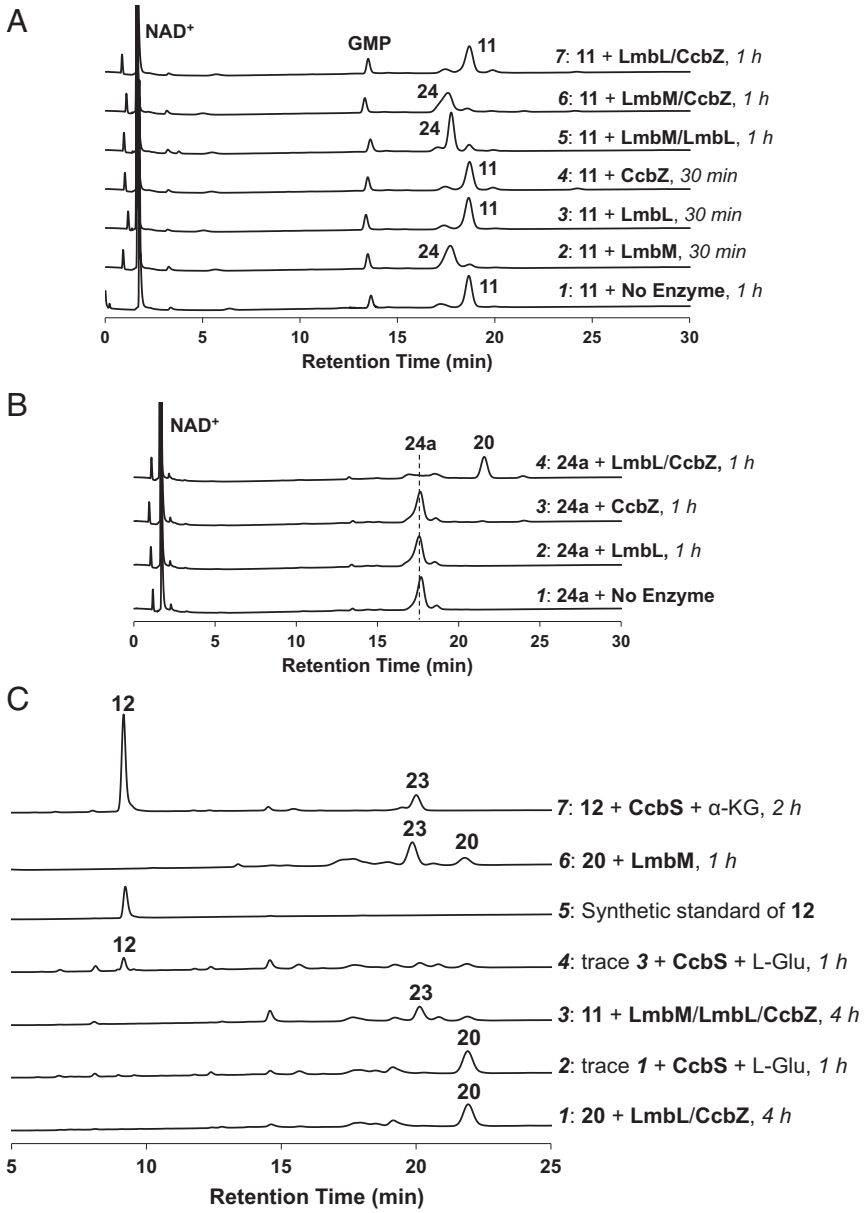

Fig. 3. (*A*) HPLC analysis of LmbM, LmbL, and CcbZ reactions using GDP-octose (**11**) as the substrate (product **24** was later determined to be **24a**). (*B*) HPLC analysis of LmbL and CcbZ reactions using **24a** as substrate. All reaction mixtures contain NAD^+. (*C*) HPLC analysis of CcbS activity on **20** and **23** generated from **11** through LmbM/LmbL/CcbZ catalysis (traces *1* to *4*), LmbM activity on **20** (trace *6*), and the reverse transamination reaction catalyzed by CcbS using **12** as the substrate (trace *7*). Reaction mixtures in traces *1 to 4* and *6* contain NAD^+.

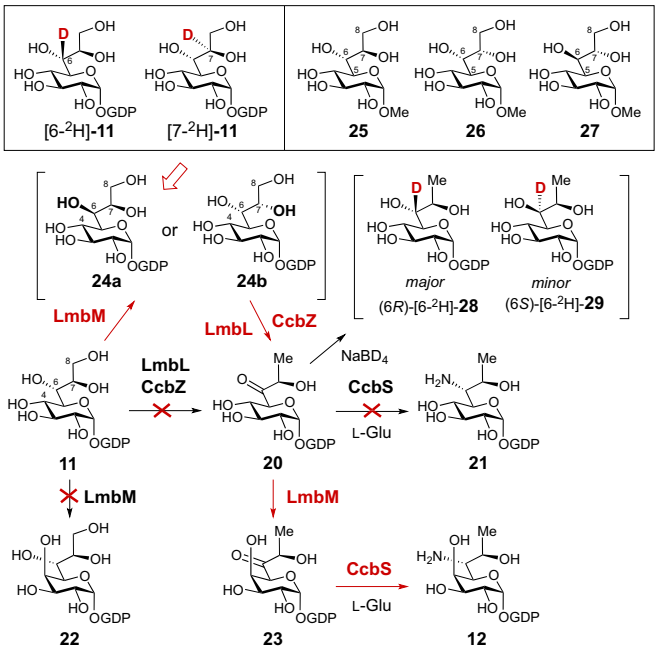

Fig. 4. The enzymatic conversion of **11** to **12** (D = ^{2}H shown in structures).

C6 and C7 in the products derived from [6-^{2}H]-**11** and [7-^{2}H]-**11**, respectively, was noted after the LmbM-catalyzed isomerization (*SI Appendix*, Figs. S5 and S10). This allowed assignment of the coupling constants $J_{5,6}$, $J_{6,7}$, $J_{7,8a}$, and $J_{7,8b}$ of the LmbM product to values of ~0, ~0, 3.5, and 6.5 Hz, respectively (*SI Appendix*, Figs. S4 and S5). In parallel, methyl α-D-*gluco*-octopyranosides **25**, **26,** and **27** were also synthesized (*SI Appendix*, S2.4–S2.6) as model analogs for comparison with the LmbM product. The $J_{5,6}$ coupling constants in **25**, **26,** and **27** were found to be 2.5, 4.0, and ~0 Hz, respectively (*SI Appendix*, Fig. S3). Because $J_{5,6}$ is ~2.4 to 4.0 Hz in **11**, **25,** and **26** (6*R* stereochemistry) versus roughly 0 Hz in **27** (6*S* stereochemistry), the observed value of $J_{5,6}$ = ~0 Hz in the LmbM product suggested 6*S* stereochemistry and assignment as the C6-epimerized octose **24a**.

Since compound **24a** generated by LmbM is the first enzymatic product from **11**, it should be the substrate for the next step in the pathway to **12**. As shown in Fig. 3*B*, while **24a** is inert to LmbL or CcbZ alone, it could be metabolized by a 1:1 molar mixture of LmbL and CcbZ to yield a product that has an HPLC retention time of ~22.0 min (Fig. 3*B*, trace *4*). This compound was determined to be **20** because reduction with $NaBD_4$ resulted in formation of (6*R*)-[6-^{2}H]-**28** as the major reduced product based on NMR and mass spectrometry analysis (*SI Appendix*, Figs. S6–S8). Although LmbL and CcbZ together are capable of catalyzing dehydration of **24a**, the same is not true for **11** (Fig. 3*A*, trace *7*). These findings ruled out a direct transformation of **11** to **20** and underscored the importance of the LmbM-catalyzed epimerization of **11** to **24a** in the pathway (Fig. 4).

Incubation of **20** with CcbS, PLP, and L-glutamate (Fig. 3*C*, trace *2*) did not lead to the anticipated transamination (*Materials and Methods*). This is inconsistent with a route involving direct turnover of **20** to **21**, but instead suggests a model in which **23** is likely the substrate for CcbS (Figs. 2*B* and 4). It was also noted that successful conversion of **11** to **12** was achieved when **11** was first treated with a mixture of LmbM, LmbL, and CcbZ (1:1:1 molar ratio) followed by the addition of CcbS (Fig. 3*C*, traces *3* and *4*). The identity of the overall enzymatic product was confirmed to be GDP-D-α-D-lincosamide (**12**) by comparing it with the synthesized standard (*SI Appendix*, S2.2). Thus, transformation of **11** to **23** is possible with only LmbM, LmbL, and CcbZ, implying that LmbM catalyzes the epimerization not only of C6 in **11** but also of C4 in **20**. This is consistent with the observation that **23** could be produced during the incubation of **20** with LmbM alone (Fig. 3*C*, trace *6*). To further confirm that **23** is the immediate precursor to **12**, the CcbS-catalyzed transamination reaction was run in the biosynthetic reverse direction using the prepared standard of **12** as the substrate. Incubation of **12** with CcbS, PLP, and α-ketoglutarate showed the appearance of a product peak (Fig. 3*C*, trace *7*) that shared the same retention time and molecular weight as **23** (calcd *m/z* for $C_{18}H_{27}O_{17}N_5P_2^-$ $[M-H]^-$: 646.0804, found 646.0760). This is consistent with the finding that LmbM, LmbL, and CcbZ catalyze the conversion of **11** to **23** as the immediate precursor to **12**. Taken together, the collective results strongly suggest that the transformation of **11** to **12** proceeds in the sequence of **11** → **24a** → **20** → **23** → **12** (Figs. 2*B* and 4 and *SI Appendix*, Fig. S8).

Reaction Catalyzed by LmbM. LmbM is related to two well-studied epimerases, namely, ADP-L-*glycero*-D-*manno*-heptose-6-epimerase (AGME) (21%[I]/33%[S]) (38–40) and UDP-D-galactose 4-epimerase (GALE) (32% [I]/47%[S]) (34–37) (*SI Appendix*, Table S3). AGME catalyzes the interconversion between ADP-D-*glycero*-β-D-*manno*-heptose **30** and ADP-L-*glycero*-β-D-*manno*-heptose **31** during the biosynthesis of lipopolysaccharides and heptose antibiotics and thus operates as a C6 epimerase (Fig. 5) (38–40). In contrast, GALE is a C4 epimerase that catalyzes the interconversion of UDP-α-D-glucose **32** and UDP-α-D-galactose **33** in the Leloir pathway of galactose metabolism (34–36). Sequence analysis shows that all three enzymes have an NAD^+-binding motif GxxGxxG characteristic of members of the short-chain dehydrogenase/reductase family (37) and a YxxxK motif believed to be important for interactions with the 4-hydroxyl group of the NDP-pyranose sugar substrate (*SI Appendix*, Fig. S9) (41–43).

The structures of AGME and GALE are highly similar despite differences in their regioselectivity (39, 41–43). LmbM, GALE, and AGME thus represent three related epimerases that utilize a tightly bound NAD^+ cofactor to catalyze epimerization of the C4 or C6 positions. Release of NAD^+/NADH was indeed observed when purified LmbM was denatured (*SI Appendix*, Fig. S12). The reactions catalyzed by GALE and AGME have been established to be initiated by oxidation of C4-OH or C6-OH of the respective substrate to yield a keto-sugar intermediate with concomitant reduction of the bound NAD^+. This is followed by a conformational change via bond rotation to expose the opposite

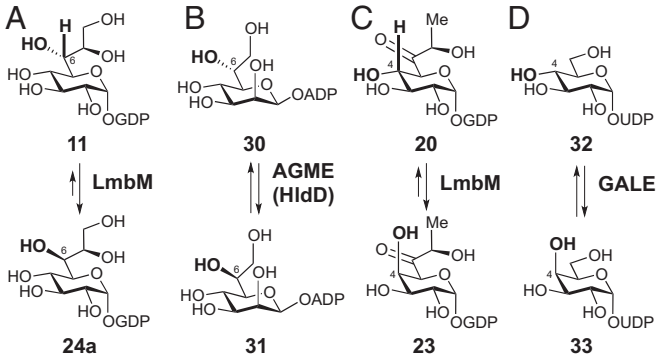

Fig. 5. (*A*) LmbM-catalyzed 6-epimerization of **11** to **24a**. (*B*) AGME-catalyzed 6-epimerization of ADP-D-*glycero*-β-D-*manno*-heptose (**30**) to **31**. (*C*) LmbM-catalyzed 4-epimerization of **20** to **23**. (*D*) GALE-catalyzed 4-epimerization between UDP-α-D-glucose (**32**) and UDP-α-D-galactose (**33**).

face of the keto group to the NADH factor to facilitate hydride transfer with inversion of the stereochemistry at C4 or C6 in the corresponding product (35, 36). A similar mechanism is also expected for the LmbM-catalyzed reactions. LmbM is unique, however, in that it exhibits both C4 and C6 epimerase activities depending on the substrate. Interestingly, the reaction of GALE requires a flipping over of the pyranose ring along the anomeric C-O-P bond (35, 41–43), whereas that of AGME requires rotation of the C6 carbonyl about the C5-C6 bond (40). The fact that LmbM can catalyze epimerization at both C4 (GALE-like activity) and C6 (AGME-like activity) is rather unusual given the dramatic differences in the reorientations required for a direct oxidation/reduction mechanism.

Mechanisms of LmbL/CcbZ-Catalyzed Dehydration. LmbL and CcbZ together catalyze a redox-neutral 6,8-dehydration; however, it is unclear what role each gene product plays in this reaction. While NDP-sugar 4,6-dehydratases are prevalent in nature, they are generally represented by an enzyme encoded in a single open reading frame (ORF) (44–48). Furthermore, the mechanism of LmbL/CcbZ-catalyzed 6,8-dehydration is expected to be similar to that observed among other NDP-sugar 4,6-dehydratases; however, there are four principal pathways by which catalysis may proceed as shown in Fig. 6. In each case, the first step is oxidation of **24a** in order to facilitate the elimination of water, and two oxidation pathways are possible depending on whether dehydrogenation takes place at C6 or C7 (routes A and B). Subsequent enolization would lead to the common intermediate **36,** which could undergo 6,8-elimination to generate **37** prior to reduction that may again proceed via one of two possible pathways (i.e., routes C and D, respectively).

To investigate these mechanistic hypotheses, the chemically synthesized LmbM substrate isotopologues, GDP-[6-^{2}H]-D-*erythro*-α-D-*gluco*-octose ([6-^{2}H]-**11**) and GDP-[7-^{2}H]-D-*erythro*-α-D-*gluco*-octose ([7-^{2}H]-**11**), were incubated with LmbM to prepare labeled LmbM products [6-^{2}H]-**24a** and [7-^{2}H]-**24a**, which were used as mechanistic probes to study the LmbL/CcbZ-catalyzed 6,8-dehydration. When GDP-[6-^{2}H]-D-*threo*-α-D-*gluco*-octose ([6-^{2}H]-**24a**) was incubated with LmbL and CcbZ, the enzymatic product showed a mass signal ([M – H]$^-$ = 646.0790) that matched the unlabeled **20** ([M – H]$^-$ calculated as 646.0804) (*SI Appendix*, Fig. S10), indicating loss of the [6-^{2}H] label. The proton NMR spectrum of the major $NaBD_4$-reduced derivative of this product (Fig. 6*B*, spectrum 2) matches well with that of [6-^{2}H]-**28** generated from the unlabeled **24a** under the same conditions (Fig. 6*B*, spectrum 1). Conversely, the LmbL/CcbZ product obtained from [7-^{2}H]-**24a** gave a *m/z* signal of [M – H]$^-$ = 647.0837, indicating retention of the C7-D label in **20**. Furthermore, the deuterium label remained at C-7 in **28** according to proton NMR following reduction of the C6 ketone with $NaBD_4$, which resulted in a silent H-7 signal and the C8-Me collapsing to a singlet (Fig. 6*B*, spectrum 3). These findings are

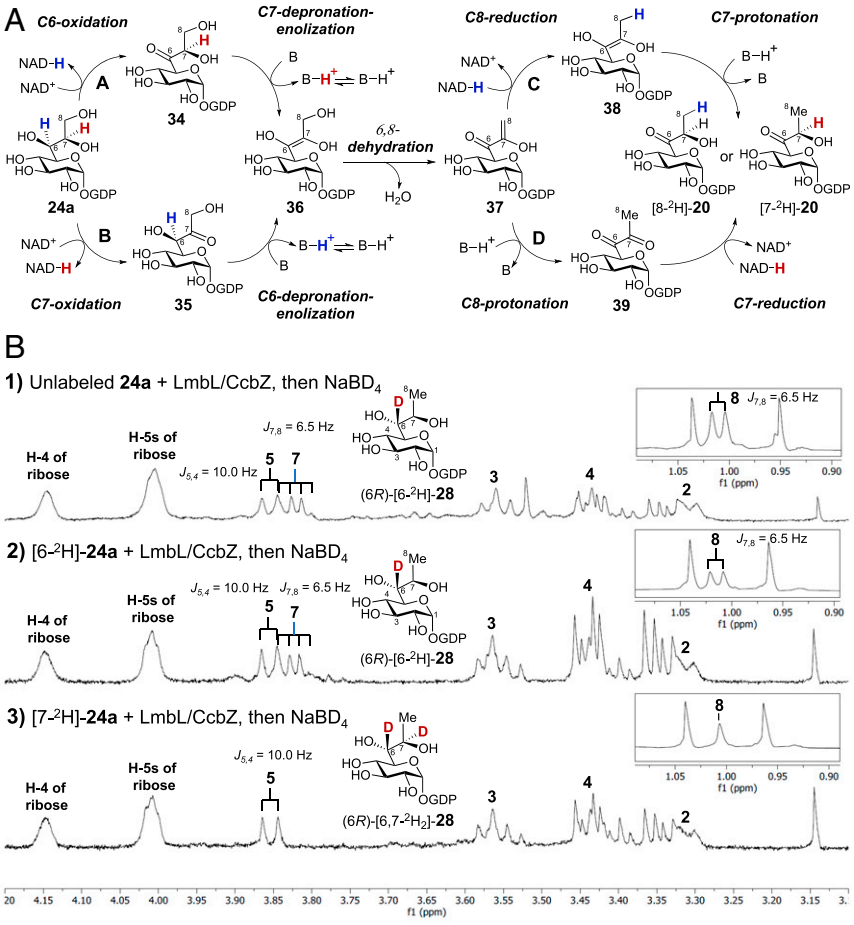

Fig. 6. (*A*) Proposed mechanisms of LmbL/CcbZ-catalyzed 6,8-dehydration. Only the fate of the colored deuteride in the reduced NAD coenzyme generated in the first-half reaction is followed in the second-half reaction. (*B*) Comparison of proton NMR spectra of the major products derived from the incubation of **24a** (spectrum 1), [6-^{2}H]-**24a** (spectrum 2), and [7-^{2}H]-**24a** (spectrum 3) with LmbL/CcbZ followed by $NaBD_4$ reduction (D = ^{2}H shown in structures). Peaks from impurities were difficult to remove since the samples were prone to degradation upon repeated purification.

consistent with a mechanism in which the 6,8-dehydration is initiated by dehydrogenation of the C7-hydroxyl by the active-site NAD^+ cofactor, elimination of water, and C7 reduction by the reduced active-site NADH cofactor to complete the catalytic cycle (**24a** → **35** → **36** → **37** → **39** → **20**, route B followed by route D in Fig. 6*A*).

Since the *lmbL* and *lmbZ* gene products display sequence homology to UDP-D-glucose/GDP-D-mannose 6-dehydrogenase and NAD(P)-dependent oxidoreductase, respectively, either LmbL or CcbZ could be directly responsible for the redox reactions underlying the conversion of **24a** to **20**. However, sequence alignment of LmbL, CcbL, LmbZ, and CcbZ with known NDP-hexose 4,6-dehydratases (*SI Appendix*, Fig. S11) revealed the absence of a YxxxK motif in these enzymes, which is consistent with no LmbL/CcbZ activity on the pyranose core of **24a**. Moreover, LmbL and CcbL lack the GxxGxxG NAD^+-binding motif that is conserved in all NDP-hexose 4,6-dehydratases, while both LmbZ and CcbZ contain the uncommon GxxWxxG motif at the N terminus that may still serve to bind an NAD^+ cofactor. To test this hypothesis, LmbL and CcbZ were separately denatured, and the respective supernatants were analyzed by liquid chromatography–mass spectrometry for the presence of released cofactor. As expected, no NAD^+/NADH was found to be discharged from the denatured LmbL, whereas CcbZ was found to release NAD^+/NADH (*SI Appendix*, Fig. S12). These observations imply that CcbZ may be the catalytic component directly responsible for dehydrogenation of the C7-hydroxyl group in **24a** and subsequent C7 reduction of the putative intermediate **39**.

Initial dehydrogenation at the C7 position of **24a** catalyzed by CcbZ presumably necessitates tautomerization to an enediol intermediate such as **36** prior to a 1,4-dehydration (**36** → **37**) as shown in Fig. 7*A*. Since LmbL is also required for the 6,8-dehydration reaction, it may play a role in tautomerization and dehydration (**35** → **36** → **37** → **39**). This stands in contrast to the more direct 1,2-dehydration (**42** → **43**) that has generally been suggested for the NDP-sugar 4,6-dehydratases (Fig. 7*B*) (44–48).

In the case of the 4,6-dehydratases, deprotonation at C5 of **42** leads to an α-carbanion in conjugation with the adjacent carbonyl at C4 effectively forming an enolate intermediate (not shown) during what amounts to an E1cb-type dehydration. However, in view of the mechanism proposed for LmbL/CcbZ (Fig. 7*A*), deprotonation at C5 catalyzed by NDP-sugar 4,6-dehydratases could alternatively result in a tautomerization reaction (**42** → **44**) prior to a 1,4-dehydration (**44** → **43**) (Fig. 7*B*). In contrast, tautomerization to the enediol intermediate **36** appears to be necessary in the catalytic cycle of LmbL/CcbZ because **35** has no abstractable α-proton at C7. Thus, the dehydration catalyzed by LmbL/CcbZ represents a 1,4-elimination that has not been previously reported.

Conclusion

In summary, four enzymes—LmbM, LmbL, CcbZ (LmbZ equivalent), and CcbS (LmbS equivalent)—have been shown to catalyze the conversion of **11** to GDP-D-α-D-lincosamide (**12**) during the biosynthesis of lincomycin. This pathway involves C6-epimerization of **11** to **24a** catalyzed by LmbM, dehydration of **24a** to **20** catalyzed by LmbL/CcbZ (i.e., LmbL/LmbZ), C4-epimerization of **20** to **23** also catalyzed by LmbM, and finally the CcbS (i.e., LmbS) catalyzed transamination of **23** to **12** as shown in Fig. 4. There are several features of this pathway that are of particular interest and hence distinguish it from other biosynthetic/metabolic pathways involving the epimerization and α,γ-dehydration of carbohydrate molecules. First, LmbM catalyzes epimerization at either the C6 or C4 position depending on the structural features of its GDP-octose substrate. This unusual catalytic property separates it from the related epimerases AGME and GALE, which appear to be much more regiospecific (38–42). Interestingly, both the C6- as well as the C4-epimerization reactions catalyzed by LmbM (as well as AGME and GALE) involve hydride abstraction from the substrate and return back to the resulting oxidized intermediate at the same site to effect the change in stereochemistry. Thus, while the regiochemistry of the LmbM-catalyzed reaction appears to be substrate specific, the overall hydride transfer remains faithfully "site" specific. Furthermore,

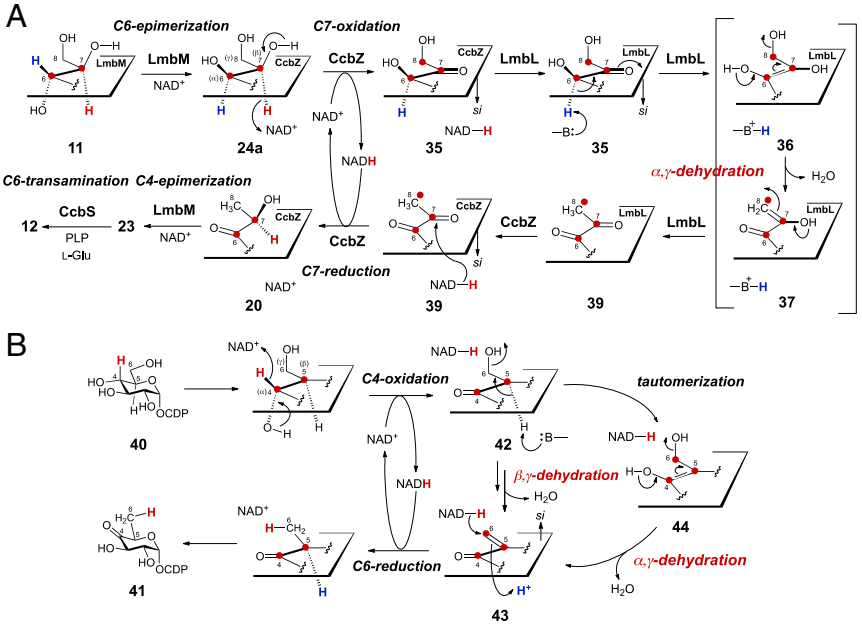

Fig. 7. (*A*) Established pathway for the conversion of **11** to **12** in the lincomycin biosynthesis. Reactions catalyzed by LmbM, CcbZ, and LmbL for the conversion of **24a** to **20** are highlighted. The labeled carbons (C6, C7, and C8) in **35** to **39** are coplanar with C7 which has a sp^2 configuration. The NAD^+ coenzyme in the active site of CcbZ is likely located at the *si* face of the above plane (see **35**, **39**). (*B*) Reaction catalyzed by CDP-α-D-glucose 4,6-dehydratase. The labeled carbons (C4, C5, and C6) in **43** and **44** are also expected to be coplanar.

although C4-epimerization during lincomycin biosynthesis is required for achieving the D-*galacto*-pyranose configuration observed in the final octose core, the intermediary C6-epimerziation is also necessary to facilitate the subsequent dehydration of **24a** to **20** catalyzed by LmbL/CcbZ.

Also of interest is the observation that the subsequent α,γ-dehydration reaction (**24a** → **20**, Fig. 7*A*) requires two gene products (LmbL and CcbZ) for activity rather than one as is typical of NDP-sugar α,γ-dehydratases (i.e., 4,6-dehydratases) (44–48). While the exact roles played by each of these components in the dehydration reaction remain to be fully elucidated, only CcbZ is expected to be directly responsible for the underlying redox reactions that involve NAD^+-mediated hydride transfer from and return to the C7 alcohol/ketone. The LmbL/CcbZ-catalyzed reaction is thus mechanistically unique as it proceeds via dehydrogenation of the hydroxyl group at the β-carbon (C7) rather than at the α-carbon (C6) as is commonly noted (e.g., **40** → **42**, Fig. 7*B*). This finding distinguishes LmbL/CcbZ from the NDP-sugar 4,6-dehydratases such as CDP-α-D-glucose 4,6-dehydratase (49, 50), which involve net hydride transfer from the α-position to the γ-position (C4 to C6) during the dehydration of **40** to **41** (Fig. 7*B*). Thus, while these results raise questions regarding the detailed chemistry of the NDP-sugar dehydratases and epimerases in general, they have finally completed the description of the lincomycin biosynthetic pathway and serve to highlight the complex mechanistic subtleties associated with the biosynthesis of atypical carbohydrate natural products.

Materials and Methods

Materials and Bacterial Strains. The bacterial strains of *Streptomyces lincolnensis* NRRL ISP-5355 (identical to ATCC 25466) and *Streptomyces caelestis* NRRL-2418 were obtained from the Agricultural Research Service Culture Collection of the National Center for Agricultural Utilization Research. *E. coli* DH5α, acquired from Bethesda Research Laboratories, was used for routine cloning experiments. The protein overexpression host *E. coli* BL21 star (DE3) was obtained from Invitrogen. Vectors for protein overexpression were purchased from Novagen. All chemicals and reagents were purchased from Sigma-Aldrich Chemical or Fisher Scientific and were used without further purification. Oligonucleotide primers were prepared by Integrated DNA Technologies. Kits for DNA gel extraction and spin minipreps were purchased from Qiagen. PureLink Genomic DNA Mini Kit was obtained from Invitrogen. *Thermococcus kodakaraensis* (KOD) DNA polymerase was purchased from Novagen. A QuikChange site-directed mutagenesis kit was obtained from Stratagene (later acquired by Agilent). Enzymes and molecular weight standards used for the cloning experiments were obtained from New England Biolabs. Reagents for SDS polyacrylamide gel electrophoresis (SDS/PAGE) were purchased from Bio-Rad, except the protein molecular weight markers, which were obtained from Invitrogen. Growth medium components were acquired from Becton Dickinson. Sterile syringe filters are products of Fisher Scientific. Amicon YM-10 ultrafiltration membranes were bought from Millipore. The analytical and semipreparative CarboPac PA1 HPLCy (HPLC) columns were obtained from Dionex. Analytical C-18 HPLC columns were products of Varian. Semipreparative C-18 HPLC columns were purchased from Fisher Scientific.

General Cloning and Expression of Enzymes. Standard genetic manipulations of *E. coli* were performed as described by Sambrook and Russell (51). DNA sequencing was performed at the core facility of the Institute of Cellular and Molecular Biology, The University of Texas at Austin. DNA concentrations were measured using a NanoDrop ND-1000 UV-vis instrument from Thermo Fisher Scientific. Target genes *lmbL*, *lmbM*, *ccbS*, and *ccbZ* were amplified from their corresponding genomic DNA isolated from *S. lincolnensis* and *S. caelestic* using designed primer pairs, and they were cloned into pET24b(+), pET28b(+), and pET-MalE vectors (*SI Appendix*, Table S2). The resulting plasmids were used to transform *E. coli* BL21 Star (DE3) cells. The desired enzymes were overexpressed and purified from *E. coli* according to the following procedure. The overnight culture grown at 37 °C in 10 mL of Luria broth medium containing kanamycin (30 μg/mL) was used to inoculate 1 L of the same medium in a 100-fold dilution. These cultures were incubated at 37 °C with 200 rpm shaking until OD_{600} reached 0.5. Protein expression was induced by the addition of isopropyl β-D-1-thiogalactopyranoside to a final concentration of 0.1 mM (adjusted to 50 μM for maltose-binding protein [MBP]-fused CcbS). After overnight incubation at 18 °C with 125 × *g* shaking, the cells were harvested by centrifugation at 4,500 × *g* for 15 min, resuspended in 20 mL of 50 mM Tris(hydroxymethyl)-aminomethane (Tris) buffer (pH 8.0) containing 300 mM NaCl, 10 mM imidazole, and glycerol (10%, vol/vol), and disrupted by sonication. For CcbS isolation, excess PLP (1 mM) was added to the lysis buffer to aid the folding process of CcbS. Cell debris was removed by centrifugation at 20,000 × *g* for 20 min, and the supernatant was mixed by slow agitation with nickel-nitrilotriacetic acid (Ni-NTA) resin for 2 h at 4 °C. The slurry was transferred to a column and washed with 100 mL of 50 mM Tris buffer (pH 8.0) containing 300 mM NaCl, 20 mM imidazole, and glycerol (10%, vol/vol). The protein was eluted with 25 mL of 50 mM Tris buffer (pH 8.0) containing 300 mM NaCl, 250 mM imidazole, and glycerol (10%, vol/vol). The pooled protein fractions were dialyzed three times against 1 L of 50 mM Tris buffer (pH 8.0) containing 300 mM NaCl and 15% glycerol prior to storage at −80 °C. The CcbS protein without His_6-tag was obtained by in vitro tobacco etch virus (TEV) protease cleavage of the MBP from the MBP-CcbS fusion protein. Specifically, 5% (vol/vol) His_6-tagged TEV protease was added to the solution containing purified MBP-CcbS to cleave the His_{10}-MBP. The digestion was carried out for 24 h during dialysis. The protein mixture was then filtered through a pad of Ni-NTA resin twice to remove His-tagged MBP and TEV. The Ni-NTA pad was further washed with a two-column volume of 50 mM Tris buffer (pH 8.0) containing 300 mM NaCl, 20 mM imidazole, and glycerol (10%, vol/vol), and all protein containing filtrates were combined and concentrated with an Amicon ultra-15 centrifugal filter unit with a 10-kDa cutoff prior to storage at −80 °C. The molecular mass and purity of all purified enzymes were determined by SDS/PAGE analysis (*SI Appendix*, Fig. S1).

Chemical Synthesis. The chemical synthesis and structures of **11, 12**, **22**, [6-^{2}H]-**11,** and [7-^{2}H]-**11** are described in *SI Appendix*, S2.1–S2.3, S2.7, and S2.8.

General HPLC Elution Conditions. Purification of GDP-octoses and HPLC analysis of the enzymatic products was performed using a Dionex CarboPac PA1 analytical column (1 mL/min flow rate) or a Dionex CarboPac PA1 semipreparative column (4 mL/min flow rate) with UV absorbance detection at 254 nm. Gradient elution was performed under a two-solvent system with H_2O as solvent A and 1.0 M $NH_4OAc_{(aq)}$ as solvent B under the following conditions: 0 to 2 min of 10% solvent B, 2 to 10 min of 10 to 50% solvent B, 10 to 25 min of 50 to 90% solvent B, 25 to 27 min of 90% solvent B, and 27 to 30 min of 90 to 10% solvent B.

General Screening for Enzymatic Activity. Enzymatic activity of a specific substrate was assayed by mixing 100 μM of the compound being tested and 50 μM NAD^+ with 2.5 μM enzyme or combination of enzymes in 100 mM Tris buffer (pH 8.0) at room temperature for 30 min or 1 h. After incubation, the enzymes were removed by centrifugal filtration using YM-10 filters. The filtrate was analyzed by HPLC using a Dionex CarboPac PA1 analytical column.

CcbS Activity Assay. The putative substrate was incubated with CcbS protein (33 μM), L-glutamate (2 mM), and PLP (66 μM) in 100 mM Tris buffer (pH 8.0) at room temperature for 1 h. After the removal of proteins by centrifugal filtration using YM-10 filters, the filtrate was analyzed by HPLC using a Dionex CarboPac PA1 analytical column.

Reverse Transamination of GDP-D-α-D-Lincosamide (12) by CcbS. Synthetic GDP-D-α-D-lincosamide **12** (66 μM) (*SI Appendix*, S2.2) was incubated with CcbS (33 μM), α-ketoglutarate (2 mM), and PLP (66 μM) in 100 mM Tris buffer (pH 8.0) at room temperature for 2 h. After incubation, the enzymes were removed by centrifugal filtration using YM-10 filters. The filtrate was analyzed by HPLC using a Dionex CarboPac PA1 analytical column.

Reduction of Enzymatic Reaction Products with $NaBD_4$ or $NaBH_4$. After incubation, the enzymes were removed by centrifugal filtration using YM-10 filters. The filtrate was then incubated with 5 mM $NaBD_4$ or $NaBH_4$ in ddH_2O for 30 min, and the reaction was quenched with acetone. The resulting mixture was analyzed by HPLC using a Dionex CarboPac PA1 analytical column, and the products were purified using a Dionex CarboPac PA1 semipreparative column if necessary.

Data Availability. All data associated with these studies are included in the main text or *SI Appendix*.

ACKNOWLEDGMENTS. Portions of the paper were developed from the thesis of C.-I.L. (2015) and the thesis of S.-A.W. (2019), The University of Texas at Austin. This work was supported by grants from the NIH (GM035906) and the Welch Foundation (F-1511). The Bruker AVANCE III 500 NMR at The University of Texas at Austin was supported by the NSF (1 S10 OD021508-01).

1. D. J. Mason, A. Dietz, C. DeBoer, Lincomycin, a new antibiotic. I. Discovery and biological properties. *Antimicrob. Agents Chemother.* **1962**, 554–559 (1962).
2. R. R. Herr, M. E. Bergy, Lincomycin, a new antibiotic. II. Isolation and characterization. *Antimicrob. Agents Chemother.* **1962**, 560–564 (1963).
3. C. Lewis, H. W. Clapp, J. E. Grady, In vitro and in vivo evaluation of lincomycin, a new antibiotic. *Antimicrob. Agents Chemother.* **1962**, 570–582 (1963).
4. D. J. Mason, C. Lewis, Biological activity of the lincomycin-related antibiotics. *Antimicrob. Agents Chemother.* **10**, 7–12 (1964).
5. H. Hoeksema *et al*., Chemical studies on lincomycin. I. The structure of lincomycin. *J. Am. Chem. Soc.* **86**, 4223–4224 (1964).
6. F. Reusser, Effect of lincomycin and clindamycin on peptide chain initiation. *Antimicrob. Agents Chemother.* **7**, 32–37 (1975).
7. M. Hanada, M. Tsunakawa, K. Tomita, H. Tsukiura, H. Kawaguchi, Antibiotic Bu-2545, a new member of the celesticetin-lincomycin class. *J. Antibiot. (Tokyo)* **33**, 751–753 (1980).
8. S. Toda, S. Nakagawa, T. Naito, H. Kawaguchi, Structure of antibiotic Bu-2545, a new member of the celesticetin-lincomycin class. *J. Antibiot. (Tokyo)* **34**, 596–599 (1981).
9. H. Hoeksema, G. F. Crum, W. H. DeVries, Isolation and purification of celesticetin. *Antibiot. Annu.* **1955**, 837–841 (1954).
10. H. Hoeksema, V. Celesticetin, Celesticetin. V. The structure of celesticetin. *J. Am. Chem. Soc.* **90**, 755–757 (1968).
11. F. Schlünzen *et al*., Structural basis for the interaction of antibiotics with the peptidyl transferase centre in eubacteria. *Nature* **413**, 814–821 (2001).
12. T. Tenson, M. Lovmar, M. Ehrenberg, The mechanism of action of macrolides, lincosamides and streptogramin B reveals the nascent peptide exit path in the ribosome. *J. Mol. Biol.* **330**, 1005–1014 (2003).
13. S. Padberg, *Anti-Infective Agents: Drug During Pregnancy and Lactation*, (Elsevier, Amsterdam, ed. 3, 2015), Vol. chap. 2, pp. 115–176.
14. C.-I. Lin, R. M. McCarty, H.-w. Liu, The biosynthesis of nitrogen-, sulfur-, and high-carbon chain-containing sugars. *Chem. Soc. Rev.* **42**, 4377–4407 (2013).
15. E. Sasaki, C.-I. Lin, K.-Y. Lin, H.-w. Liu, Construction of the octose 8-phosphate intermediate in lincomycin A biosynthesis: Characterization of the reactions catalyzed by LmbR and LmbN. *J. Am. Chem. Soc.* **134**, 17432–17435 (2012).
16. C.-I. Lin, E. Sasaki, A. Zhong, H.-w. Liu, In vitro characterization of LmbK and LmbO: Identification of GDP-D-*erythro*-α-D-*gluco*-octose as a key intermediate in lincomycin A biosynthesis. *J. Am. Chem. Soc.* **136**, 906–909 (2014).
17. Q. Zhao, M. Wang, D. Xu, Q. Zhang, W. Liu, Metabolic coupling of two small-molecule thiols programs the biosynthesis of lincomycin A. *Nature* **518**, 115–119 (2015).
18. D. Zhang, Z. Tang, W. Liu, Biosynthesis of lincosamide antibiotics: Reactions associated with degradation and detoxification pathways play a constructive role. *Acc. Chem. Res.* **51**, 1496–1506 (2018).
19. U. Peschke, H. Schmidt, H.-Z. Zhang, W. Piepersberg, Molecular characterization of the lincomycin-production gene cluster of *Streptomyces lincolnensis* 78-11. *Mol. Microbiol.* **16**, 1137–1156 (1995).
20. M. Koberská *et al*., Sequence analysis and heterologous expression of the lincomycin biosynthetic cluster of the type strain *Streptomyces lincolnensis* ATCC 25466. *Folia Microbiol. (Praha)* **53**, 395–401 (2008).
21. N. M. Brahme *et al*., Biosynthesis of the lincomycins. 2. Studies using stable isotopes on the biosynthesis of methylthiolincosaminide moiety of lincomycin A. *J. Am. Chem. Soc.* **106**, 7878–7883 (1984).
22. N. M. Brahme *et al*., Biosynthesis of the lincomycins. 1. Studies using stable isotopes on the biosynthesis of the propyl-and ethyl-L-hygric acid moieties of lincomycins A and B. *J. Am. Chem. Soc.* **106**, 7873–7878 (1984).
23. J. Novotná *et al*., l-3,4-Dihydroxyphenyl alanine-extradiol cleavage is followed by intramolecular cyclization in lincomycin biosynthesis. *Eur. J. Biochem.* **271**, 3678–3683 (2004).
24. J. Novotna *et al*., Lincomycin biosynthesis involves a tyrosine hydroxylating heme protein of an unusual enzyme family. *PLoS One* **8**, e79974 (2013).
25. L. Najmanová *et al*., Characterization of *N*-demethyllincosamide methyltransferases LmbJ and CcbJ. *ChemBioChem* **14**, 2259–2262 (2013).
26. J. Bauer *et al*., Structure and possible mechanism of the CcbJ methyltransferase from *Streptomyces caelestis*. *Acta Crystallogr. D Biol. Crystallogr.* **70**, 943–957 (2014).
27. P. Jiraskova *et al*., New concept of the biosynthesis of 4-alkyl-L-proline precursors of lincomycin, hormaomycin, and pyrrolobenzodiazepines: Could a γ-glutamyltransferase cleave the C–C bond? *Front. Microbiol.* **7**, 276 (2016).
28. G. Zhong, Q. Zhao, Q. Zhang, W. Liu, 4-Alkyl-L-(dehydro)proline biosynthesis in actinobacteria involves N-terminal nucleophile-hydrolase activity of γ-Glutamyltranspeptidase homolog for C-C bond cleavage. *Nat. Commun.* **8**, 1–10 (2017).
29. Z. Kamenik *et al*., C-C bond cleavage in biosynthesis of 4-alkyl-L-proline precursors of lincomycin and anthramycin cannot precede C-methylation. *Nat. Commun.* **9**, 3167 (2018).
30. G. Zhong, H. Chen, W. Liu, Reply to "C–C bond cleavage in biosynthesis of 4-alkyl-L-proline precursors of lincomycin and anthramycin cannot precede C-methylation". *Nat. Commun.* **9**, 1–3 (2018).
31. Z. Kamenik *et al*., Deacetylation of mycothiol-derived "waste product" triggers the last biosynthetic steps of lincosamide antibiotics. *Chem. Sci. (Camb.)* **7**, 430–435 (2016).
32. M. Wang, Q. Zhao, Q. Zhang, W. Liu, Differences in PLP-dependent cysteinyl processing lead to diverse *S* -functionalization of lincosamide antibiotics. *J. Am. Chem. Soc.* **138**, 6348–6351 (2016).
33. R. Ushimaru, C.-I. Lin, E. Sasaki, H.-w. Liu, Characterization of enzymes catalyzing transformations of cysteine *S*-conjugated intermediates in the lincosamide biosynthetic pathway. *ChemBioChem* **17**, 1606–1611 (2016).
34. L. F. Leloir, The enzymatic transformation of uridine diphosphate glucose into a galactose derivative. *Arch. Biochem. Biophys.* **33**, 186–190 (1951).
35. P. A. Frey, "Complex pyridine nucleotide-dependent transformations" in *Pyridine Nucleotide Coenzymes*, D. Dolphin, R. Poulson, O. Avramovic, Eds. (Wiley-Interscience, 1987), Part B, pp. 461–511.
36. H. M. Holden, I. Rayment, J. B. Thoden, Structure and function of enzymes of the Leloir pathway for galactose metabolism. *J. Biol. Chem.* **278**, 43885–43888 (2003).
37. K. L. Kavanagh, H. Jörnvall, B. Persson, U. Oppermann, Medium- and short-chain dehydrogenase/reductase gene and protein families: The SDR superfamily: Functional and structural diversity within a family of metabolic and regulatory enzymes. *Cell. Mol. Life Sci.* **65**, 3895–3906 (2008).
38. L. Ding, B. L. Seto, S. A. Ahmed, W. G. Coleman Jr., Purification and properties of the *Escherichia coli* K-12 NAD-dependent nucleotide diphosphosugar epimerase, ADP-L-glycero-D-mannoheptose 6-epimerase. *J. Biol. Chem.* **269**, 24384–24390 (1994).
39. A. M. Deacon, Y. S. Ni, W. G. Coleman Jr., S. E. Ealick, The crystal structure of ADP-L-glycero-D-mannoheptose 6-epimerase: Catalysis with a twist. *Structure* **8**, 453–462 (2000).
40. J. A. Read, R. A. Ahmed, J. P. Morrison, W. G. Coleman Jr., M. E. Tanner, The mechanism of the reaction catalyzed by ADP-β-L-*glycero*-D-*manno*-heptose 6-epimerase. *J. Am. Chem. Soc.* **126**, 8878–8879 (2004).
41. J. B. Thoden, T. M. Wohlers, J. L. Fridovich-Keil, H. M. Holden, Crystallographic evidence for Tyr 157 functioning as the active site base in human UDP-galactose 4-epimerase. *Biochemistry* **39**, 5691–5701 (2000).
42. J. B. Thoden, P. A. Frey, H. M. Holden, Molecular structure of the NADH/UDP-glucose abortive complex of UDP-galactose 4-epimerase from *Escherichia coli*: Implications for the catalytic mechanism. *Biochemistry* **35**, 5137–5144 (1996).
43. Y. Liu *et al*., Mechanistic roles of tyrosine 149 and serine 124 in UDP-galactose 4-epimerase from *Escherichia coli*. *Biochemistry* **36**, 10675–10684 (1997).
44. H.-w. Liu, J. S. Thorson, Pathways and mechanisms in the biogenesis of novel deoxysugars by bacteria. *Annu. Rev. Microbiol.* **48**, 223–256 (1994).
45. G. Samuel, P. Reeves, Biosynthesis of O-antigens: Genes and pathways involved in nucleotide sugar precursor synthesis and O-antigen assembly. *Carbohydr. Res.* **338**, 2503–2519 (2003).
46. X. M. He, H.-w. Liu, Formation of unusual sugars: Mechanistic studies and biosynthetic applications. *Annu. Rev. Biochem.* **71**, 701–754 (2002).
47. C. J. Thibodeaux, C. E. Melançon, H.-w. Liu, Unusual sugar biosynthesis and natural product glycodiversification. *Nature* **446**, 1008–1016 (2007).
48. C. J. Thibodeaux, C. E. Melançon III, H.-w. Liu, Natural-product sugar biosynthesis and enzymatic glycodiversification. *Angew. Chem. Int. Ed. Engl.* **47**, 9814–9859 (2008).
49. Y. Yu, R. N. Russell, J. S. Thorson, L. D. Liu, H.-w. Liu, Mechanistic studies of the biosynthesis of 3,6-dideoxyhexoses in *Yersinia pseudotuberculosis*. Purification and stereochemical analysis of CDP-D-glucose oxidoreductase. *J. Biol. Chem.* **267**, 5868–5875 (1992).
50. C.-T. Chang, X. H. Chen, H.-w. Liu, CDP-6-deoxy-6,6-difluoro-D-glucose, a mechanism-based inhibitor for CDP-D-glucose 4,6-dehydratase. *J. Am. Chem. Soc.* **120**, 9698–9699 (1998).
51. J. Sambrook, D. W. Russell, *Molecular Cloning: A Laboratory Mannual*, (Cold Spring Harbor Laboratory Press, ed. 3, 2001).